Synthesis and Opto-electronic Properties of a Red-Emitting Heteroleptic Platinum Complex Using Pyrazol-based Diketone Derivative as Ancillary Ligand

Deng, Jiyong[a,b](邓继勇) Wang, Yafei[a](王亚飞) Li, Xiaoshuang[a](李小双)
Ni, Meijun[a](倪美君) Liu, Ming[a](刘明) Liu, Yu*,[a](刘煜) Lei, Gangtie[a](雷钢铁)
Zhu, Meixiang[a](朱美香) Zhu, Weiguo*,[a](朱卫国)

[a] *College of Chemistry, Key Laboratory of Environment-Friendly Chemistry and Application of Ministry of Education, Xiangtan University, Xiangtan, Hunan 411105, China*
[b] *Department of Chemistry and Engineering, Hunan Institute of Engineering, Xiangtan, Hunan 411104, China*

A red-emitting heteroleptic cyclometalated platinum(II) complex containing an ancillary ligand of pyrazol-based diketone derivative was synthesized. Its optophysical and electroluminescent properties were studied. Compared to the reported (piq)Pt(acac) complex, this platinum(II) complex exhibited a blue-shifted UV absorption band at 300—450 nm, a low LUMO energy level and improved electroluminescent property. Using this platinum(II) complex as a single doping emitter and a blend of ploy(9,9-dioctylfluorene) and 2-*tert*-butylphenyl-5-phenyl-1,3,4-oxadiazole as a host matrix, the fabricated polymer light-emitting devices displayed saturated red emission with a peak at 648 nm and a shoulder at 601 nm. Furthermore, the emission quenching of the platinum(II) complex was significantly suppressed in these devices at high current density due to an introduction of the non-planar pyrazol group into the ancillary ligand.

Keywords electroluminescence, platinum(II) complex, synthesis design, molecular device, optoelectronic properties

Introduction

In the field of optoelectronic materials, cyclometalated complexes have attracted significant attention because they have strong spin-orbital coupling and can make full use of both singlet and triplet excitons to achieve a 100% internal quantum efficiency in theory.[1-14] Among these cyclometalated complexes, platinum(II) complexes have a square-planar d^8 electronic configuration, which could cause molecular aggregation leading to emission quenching. Therefore, platinum(II) complexes generally display lower luminous efficiency than the non-planar iridium complexes in organic/ polymer light-emitting devices (OLEDs/ PLEDs).[15-20]

In order to improve electroluminescence (EL) properties of platinum(II) complexes in these devices, an effective method was reported to suppress molecular aggregation and emission quenching by incorporating some bulky groups into cyclometalated ligands.[19,20] In this paper, we present another method to get the same aim via introducing a prazol group into ancillary ligand. The resulting ancillary ligand of the pyrazol-based diketone derivative is 3-methyl-1-phenyl-4-(3,4,5-trifluorobenzoyl)-1*H*-pyrazol-5(4*H*)-one (Hmptfbp) and its cyclometalated platinum(II) complex is (piq)Pt(mptfbp), in which piq is 1-phenylisoquinoline. The molecular structure and synthetic route of (piq)Pt(mptfbp) are shown in Scheme 1. Its thermal, electrochemical, optophysical and EL properties were investigated. Employing (piq)Pt(mptfbp) as a single doping emitter and a blend of ploy(9,9-dioctyl fluorene) (PFO) and 2-*tert*-butylphenyl-5-phenyl-1,3,4-oxadiazole (PBD) as a host matrix, the single-emissive-layer (SEL) PLEDs presented a saturated red emission peaked at 648 nm at different dopant concentrations from 1 wt% to 8 wt%. The maximum external quantum efficiency (QE_{ext}) of 0.7% was obtained at current density of 34.8 mA/cm^2 in the device at 4 wt% dopant concentration. Significantly, the QE_{ext} still remained a level of 0.62% while the current density increased to 100 mA/cm^2. As expected, this cyclometalated platinum(II) complex with a bulky ancillary ligand exhibited a restrainable emission quenching in PLEDs at high current density.

* E-mail: zhuwg18@126.com; liuyu03b@126.com; Tel.: 0086-0731-58298280; Fax: 0086-0731-58292251
Received December 16, 2010; revised May 5, 2011; accepted June 1, 2011.
Project supported by the National Natural Science Foundation of China (Nos. 50973093, 20772101, 20872124), Research Fund and the New Teacher Fund for the Doctoral Program of Higher Education of China (Nos. 20094301110004, 200805301013), Science Foundation of Hunan Province (No. 2009FJ2002), Scientific Research Fund of Hunan Provincial Education Department (No. 10A119, 11CY023) and the Postgraduate Science Foundation for Innovation in Hunan Province (No. CX2009B124).

Scheme 1 Synthetic route of the (piq)Pt(mptfbp) complex

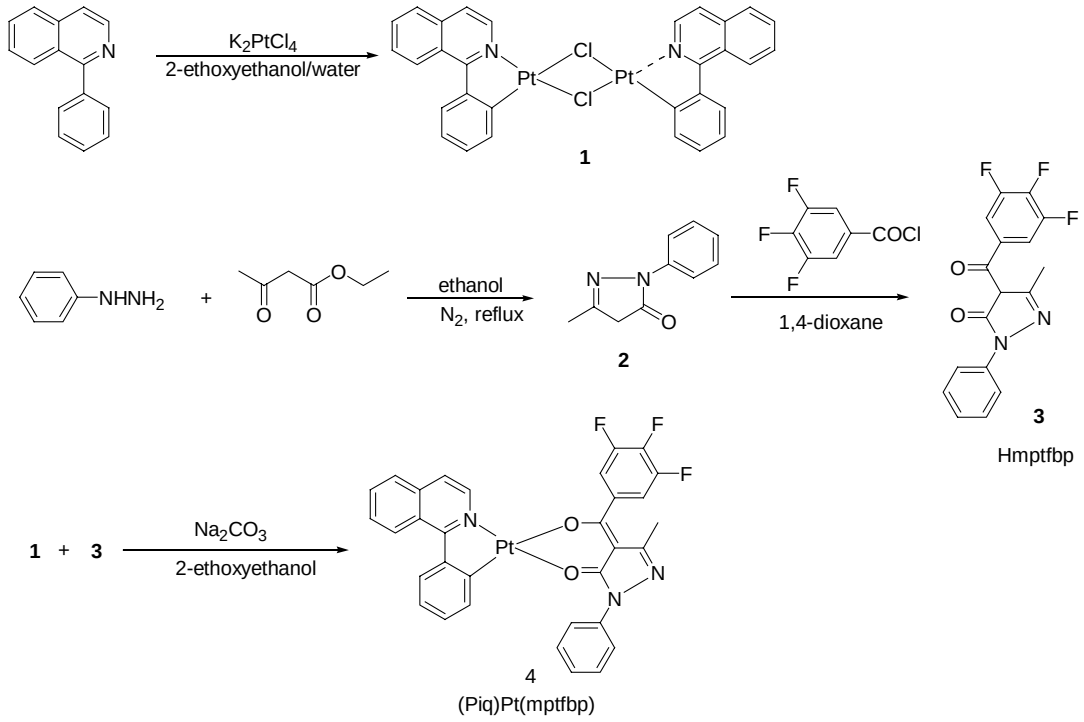

Results and discussion

Thermal property

The thermal stability of the (piq)Pt(mptfbp) and (piq)Pt(acac) complexes is evaluated by thermogravimetric analysis (TGA) under N_2 stream, and the data are summarized in Table 1. The onset decomposition temperature (T_d) for 5% weight loss is 256 ℃ for (piq)Pt(mptfbp) and 315 ℃ for (piq)Pt(acac), respectively. Therefore, this platinum(II) complex containing a pyrazol-based ancillary ligand still presents a high thermal stability.

Photophysical properties

The UV-vis absorption and photoluminescent (PL) spectra of the (piq)Pt(mptfbp) and (piq)Pt(acac) complexes in dichloromethane (DCM) at room temperature are shown in Figure 1 and their data are listed in Table 1. For the (piq)Pt(mptfbp) complex, two typical absorption bands are observed at about 306 and 412 nm, in which the former band is attributed to the ligand center-based π-π* electronic transition and the latter one is assigned to the metal-ligand charge transfer (MLCT) electronic transition. Compared to the reported (piq)Pt(acac), this (piq)Pt(mptfbp) presented a bule-shifted UV absorption band at 300—500 nm, which results from a steric effect of the ancillary ligand by introducing a pyrazole group. However, the mptfbp ancillary ligand has a minor effect on the PL profiles. Intense red emissions for these two platinum complexes are observed with a peak at 596 nm and a shoulder at 640 nm under photo-excitation at

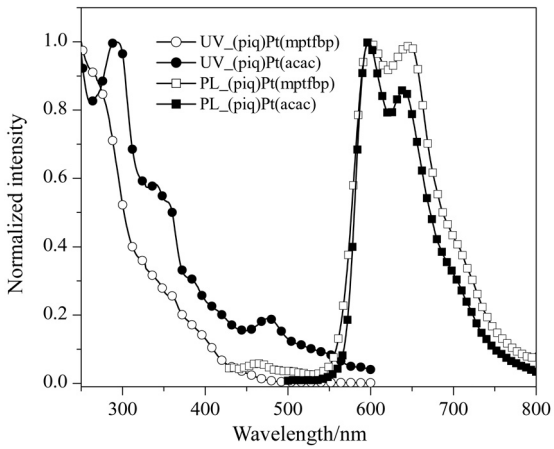

Figure 1 UV-vis absorption and PL spectra of the (piq)Pt(mptfbp) and (piq)Pt(acac) complexes in dichloromethane at 298 K.

room temperature. In order to understand the effect of ancillary ligand on PL efficiency, the PL quantum yields (Φ_f) of both platinum complexes were measured in degassed DCM at room temperature using $(piq)_2Ir(acac)$ as the standard (Φ_f = 0.2).[24] As a result, (piq)Pt(mptfbp) and (piq)Pt(acac) gave a PL quantum yield of 0.8 and 0.9, respectively. Obviously, attaching a pyrazole group into diketone ancillary ligand has a minor influence on PL efficiency of its platinum(II) complex.

The PL spectra of the (piq)Pt(mptfbp)-doped PFO-PBD films at dopant concentrations from 1 wt% to 8 wt% are shown in Figure 2. Three main emission peaks

Table 1 Optophysical and electrochemical properties of the (piq)Pt(mptfbp) and (piq)Pt(acac) complexes

Compound	UV/nm	PL/nm	E_{ox}/V	E_{HOMO}/eV	E_{LUMO}/eV	E_g/eV	T_d/℃
(piq)Pt(mptfbp)	325, 412	596, 640	0.7	−6.25	−3.74	2.50	256
(piq)Pt(acac)	290, 476	591, 643	—	−5.71	−3.23	2.48	315

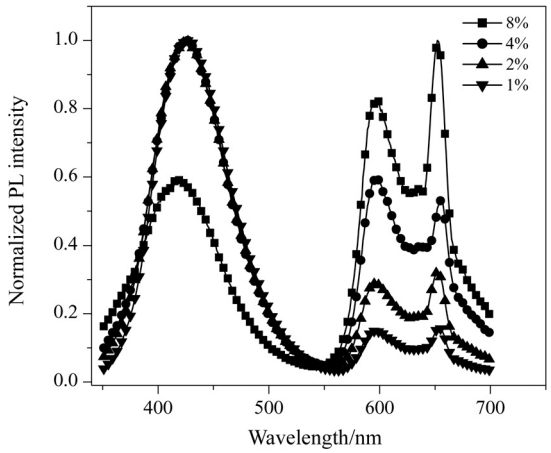

Figure 2 PL spectra of the (piq)Pt(mptfbp)-doped PFO-PBD (20%) films at different dopant concentrations from 1 wt% to 8 wt%.

at 420, 596 and 640 nm are observed, in which the high-energy peak at 420 nm results from emission of PFO-PBD host and other two low-energy peaks come from emission of the platinum(II) complex under photo-excitation. With increasing dopant concentrations, the emission from the platinum(II) complex is enhanced, but the emission from the host matrix is decreased. This implies that the energy transfer from the PFO-PBD host to the platinum(II) complex is incomplete under photo-excitation in the doped films at the dopant concentrations from 1 wt% to 8 wt%.

Electrochemical property

The electrochemical behavior of this (piq)Pt(mptfbp) complex was studied by cyclic voltammetry using ferrocene as an internal standard, and the data are listed in Table 1. A reversible oxidation wave (E_{ox}) at 0.7 V vs. a saturated calomel electrode (SCE) is observed, but the reduction wave (E_{red}) disappeared. Thus, the E_{red} was obtained based on energy band gap (E_g) and E_{ox}, in which E_g was estimated by the UV-vis absorption edge.[13] The highest occupied molecular orbital (HOMO) and the lowest unoccupied molecular orbital (LUMO) energy levels (E_{HOMO}, E_{LUMO}) of this platinum(II) complex were then calculated based on the following formula, $E_{LUMO} = -(E_{red} + 4.34)$ and $E_{HOMO} = -(E_{ox} + 4.34)$.[13] As a result, for this platinum(II) complex, E_{HOMO} and E_{LUMO} are −6.25 and −3.74 eV, respectively. Compared to (piq)Pt(acac), this complex exhibited low LUMO and HOMO energy levels.[24]

Electroluminescent property

The EL spectra of the (piq)Pt(mptfbp)-doped PFO-PBD devices at the dopant concentrations from 1 wt% to 8 wt% are shown in Figure 3. Similar EL spectra are observed in these doped devices. The maximum EL emission peak locates at 648 nm with a shoulder at 601 nm. Like the PL profiles of the (piq)Pt(mptfbp)-doped PFO-PBD films, the high-energy emission peak at 420 nm is also displayed in these EL profiles. However, this high-energy EL peak is very weak and obviously decreases with increasing dopant concentrations. While the dopant concentration increases to 4%, it almost disappears and a saturated red emission with a CIE coordinate (0.61, 0.38) is observed. Therefore, EL emissions are almost dominated by the (piq)Pt(mptfbp) dopant rather than the PFO-PBD host in the devices at the given dopant concentrations. While the dopant concentration is over 4 wt%, the emission of the PFO-PBD blend is almost quenched by the emission of (piq)Pt(mptfbp) under electricity in the devices.

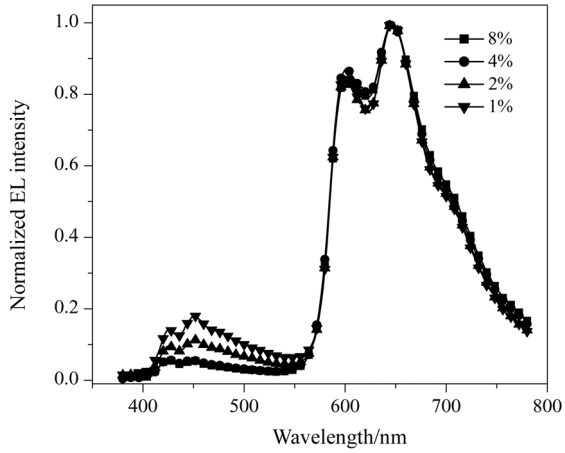

Figure 3 EL spectra of the (piq)Pt(mptfbp)-doped PFO-PBD (20%) devices at different dopant concentrations from 1 wt% to 8 wt%.

Figure 4 exhibits the current density-voltage and brightness-voltage characteristics of the (piq)Pt(mptfbp)-doped PFO-PBD devices at the dopant concentrations from 1 wt% to 8 wt%. With increasing dopant concentrations, the turn-on voltage of the devices increases from 8.75 to 14.5 V. This means that EL process in the (piq)Pt(mptfbp)-doped devices is dominated by charge trapping process besides Förster and/or Dexter transfer processes.[24]

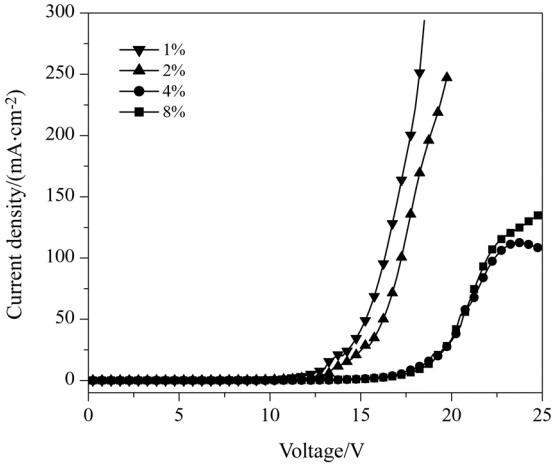

Figure 4 Current density-voltage characteristics of the (piq)Pt(mptfbp)-doped PFO-PBD (20%) devices at different dopant concentrations from 1 wt% to 8 wt%.

The external quantum efficiency-current density characteristics of the (piq)Pt(mptfbp)-doped PFO-PBD devices at the dopant concentrations from 1 wt% to 8 wt% are displayed in Figure 5. For comparison, these device performances are listed in Table 2. The maximum QE_{ext} of 0.7% at 34 mA/cm^2 and the highest brightness of 637 cd/m^2 at 247 mA/cm^2 were obtained in the device at 4 wt% dopant concentration. Further more, with increasing current density from 34 to 100 mA/cm^2, this device still exhibited a QE_{ext} as high as 0.62%. This indicates that emission quenching of this platinum(II) complex in the doped device at high current density was significantly suppressed. Introducing a non-planar pyrazol group into the diketone derivative is available to suppress emission quenching of its platinum(II) complex.

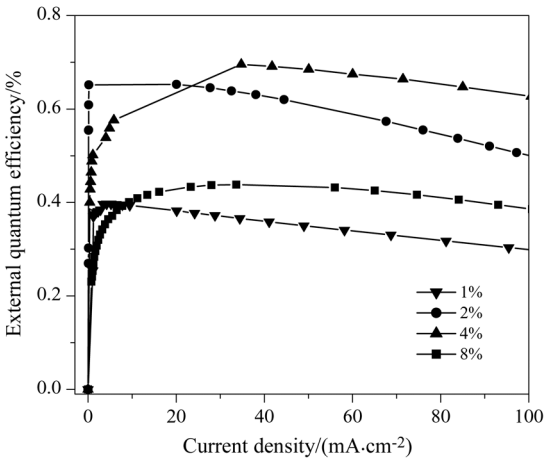

Figure 5 External quantum efficiency-current density characteristics of the (piq)Pt(mptfbp)-doped PFO-PBD (20%) devices at different dopant concentrations from 1 wt% to 8 wt%.

Conclusion

In summary, a red-emitting cyclometalated platinum(II) complex containing a pyrazol-based diketone derivative was obtained. The relation-ship between structure of platinum(II) complex and its optophysical property was primarily investigated. The emission quenching of this platinum(II) complex in its doped PLEDs was found to be efficiently suppressed although these devices have not exhibited high emission efficiency. In order to obtain higher emission efficiency, optimization of the platinum(II) complex-doped devices should be carried out.

Experimental

Physical measurements

All ^{1}H NMR spectra were acquired at a Bruker Dex-400NMR instrument using $CDCl_3$ as a solvent. Thermogravimetric analysis (TGA) was carried out with a NETZSCH STA449 instrument from 25 to 700 ℃ at a heating rate of 20 ℃/min under nitrogen atmosphere. UV-vis absorption spectra were recorded on a Perkin-Elmer Lambda 25 UV-vis absorption spectrophotometer. Photoluminescence (PL) spectra were recorded with an Insta-Spec IV CCD system (Oriel) under excitation of 325 nm line of a He-Cd laser (OmniChrome Co.). Thickness of the spin-casted film was measured with profilometer (Tencor Alfa-Step 500). Layer thickness of thermal deposition was monitored by a crystal thickness monitor (Sycon). Current density (J)-voltage (V) data were collected using a Keithley 236 source measurement unit. QE_{ext} were obtained by an integrating sphere (IS-080, Labsphere) measuring the total light output in all directions. Luminance was measured by a Si photodiode and calibrated by a PR-705 Spectrascan spectrophotometer (Photo Research). EL spectra were recorded using a CCD spectrophotometer (Instaspec 4, Oriel).

Table 2 Device performances of the (piq)Pt(mptfbp)-doped PFO-PBD (20%) devices at different dopant concentrations from 1 wt% to 8wt%

Dopants concentration	Turn-on voltage/V	Maximum brightness/(cd•m^{-2})	Maximum external quantum efficiency/%	CIE
1%	8.8	878 (19.8 V)	0.44 (33.6 mA/cm^2)	0.56, 0.35
2%	10	356 (25.2 V)	0.65 (20.0 mA/cm^2)	0.59, 0.34
4%	13.3	637 (18.5 V)	0.70 (34.8 mA/cm^2)	0.61, 0.38
8%	14.5	450 (25.5 V)	0.40 (6.3 mA/cm^2)	0.61, 0.38

Device fabrication

The phosphorescent devices using (piq)Pt(mptfbp) as dopant and a blend of PFO and PBD as a host matrix were fabricated on a clean ITO glass substrate with a sheet resistance of 15 Ω/□ (Nanbo, Shengzhen). A hole-injection layer of poly-3,4-ethylene dioxythiophene (PEDOT, 50 nm), a hole-transporting layer of poly(vinyl-carbazole) (PVK, 50 nm) and an emitting layer of platinum(II) complex doped into a PFO-PBD blend (80 nm) were spin-coated on the top of the ITO substrate successively. Subsequently, barium (4 nm) was deposited on the top of the emitting layer under vacuum (3×10^{-4} Pa) and then capped with aluminum (150 nm) by vacuum deposition. Typical active area of the devices was 0.15 mm^2 in this study. All steps except PEDOT and PVK-coating were performed in a nitrogen-filled dry glove box with oxygen and water contents less than 1×10^6.

Materials

All solvents were carefully dried and distilled prior to use. Commercially available reagents were used without further purification unless otherwise stated. 1-Phenylisoquinoline and di(1-phenylisoquinoline)-μ-chloro platinum(II) (**1**) and 3-methyl-1-phenyl-5-pyrazolone (**2**) were synthesized according to the literature procedure, respectively.[7,21-23]

Synthesis of 3-methyl-1-phenyl-4-(3,4,5-trifluorobenzoyl)-1*H*-pyrazol-5(4*H*)-one (mptfbp) (3)

A mixture of 3-methyl-1-phenyl-5-pyrazolon (3.5 g, 0.02 mol) and 1,4-dioxane (20 mL) was heated to 60 ℃ under stirring and dry anhydrous calcium hydroxide (3.0 g) was added. After strong stirring for 20 min, 3,4,5-trifluorobenzoyl chloride (4.4 g, 0.02 mol) was added dropwise into the mixture in 1 min. The reaction mixture was heated to reflux for 30 min and permitted to cool to room temperature, and then was poured into 48 mL hydrochloric acid (3 mol/L). A large number of yellow precipitate was formed and separated by filtration. The collected yellow solid was washed with alkali and water, then recrystallized from ethanol to provide yellow crystals of compound **3** (5.0 g, 73.2%). ^{1}H NMR ($CDCl_3$, 400 MHz) δ: 7.97 (d, J=4.8 Hz, 2H), 7.81 (dd, J=6.0, 7.2 Hz, 2H), 7.75 (dd, J=8.0, 7.2 Hz, 1H), 7.52 (d, J=7.2 Hz, 1H), 7.39 (d, J=4.8 Hz, 1H), 3.43 (s, 1H), 2.20 (s, 3H).

Synthesis of platinum(II) (1-phenylisoquinoline-N, $C^{2'}$) (3-methyl-1-phenyl-4-(3,4,5-trifluorobenzoyl)-1*H*-pyrazol-5(4*H*)-one-O,O) (4)

A mixture of the dimer **1** (200 mg, 0.16 mmol), 3-methyl-1-phenyl-4-(3,4,5-trifluorobenzoyl)-1*H*-pyrazol-5(4*H*)-one (**3**) (138 mg, 0.41 mmol), Na_2CO_3 (140 mg, 1.32 mmol) and 2-ethoxyethanol (20 mL) was stirred at 100 ℃ for 24 h and distilled to remove the solvent under vacuum. The residue was purified by flash chromatography using dichloromethane as an eluent to provide red solid. The red solid was recrystallized in dichloromethane/hexane to afford red crystal of compound **4** (70 mg, 30.5%). ^{1}H NMR ($CDCl_3$, 400 MHz) δ: 8.72 (d, J=6.4 Hz, 1H), 8.59 (d, J=8.0 Hz, 1H), 8.06 (d, J=6.8 Hz, 1H), 7.94 (d, J=7.2 Hz, 2H), 7.68 (d, J=6.8 Hz, 2H), 7.50 (d, J=6.8 Hz, 4H), 7.32 (d, J=6.8 Hz, 2H), 7.06—7.76 (m, 2H), 6.28—6.03 (m, 2H), 1.97 (s, 3H). Anal. calcd for $C_{32}H_{20}F_3N_3O_2Pt$: C 52.61, H 2.76, N 5.75; found C 51.98, H 2.52, N 5.78.

References

1 Lu, W. B.; Mi, X.; Chan, M. C. W.; Hui, Z.; Che, C. M. *J. Am. Chem. Soc.* **2004**, *126*, 4958.
2 Wong, W. Y.; Liu, L.; Poon, S. Y.; Choi, H. K.; Cheah, K. W.; Shi, J. X. *Macromolecules* **2004**, *37*, 4496.
3 Nakamura, A.; Tada, T.; Mizukami, M.; Yagru, S. *Appl. Phys. Lett.* **2004**, *84*, 130.
4 Hwang, F. M.; Chen, H. Y.; Chen, P. S. *Inorg. Chem.* **2005**, *44*, 1344.
5 Thomas, K. R. J.; Velusamy, M.; Lin, J. T.; Chien, C. H.; Tao, Y. T.; Wen, Y. S.; Hu, Y. H.; Chou, P. T. *Inorg. Chem.* **2005**, *44*, 5677.
6 Chang, C. Y.; Hsieh, S. N.; Wu, T. C.; Guo, T. F.; Cheng, C. H. *Chem. Phys. Lett.* **2006**, *418*, 50.
7 Lang, B.; Jiang, C. Y.; Chen, Z.; Zhang, X. J.; Shi, H. H.; Cao, Y. *J. Mater. Chem.* **2006**, *16*, 1281.
8 Wu, Z. L.; Xing, K. Q.; Luo, C. P.; Liu, L.; Yang, Y. P.; Gan, Q.; Zhu, M. X.; Jiang, C. Y.; Cao, Y. *Chin. Chem. Lett.* **2006**, *35*, 538.
9 Ho, C. L.; Wong, W. Y.; Wang, Q.; Ma, D. G.; Wang, L. X.; Lin, Z. Y. *Adv. Funct. Mater.* **2008**, *18*, 928.
10 Xu, H.; Xu, Z. F.; Yue, Z. Y.; Yan, P. F.; Wang, B.; Jia, L. W.; Li, G. M.; Sun, W. B.; Zhang, J. W. *J. Phys. Chem. C* **2008**, *112*, 15517.
11 Zhang, K.; Chen, Z.; Zou, Y.; Yang, C. L.; Qin, J. G.; Cao, Y. *Organometallics* **2007**, *26*, 3699.
12 Du, B.; Wang, L.; Wu, H. B.; Yang, W.; Zhang, Y.; Liu, R. S.; Sun, M. L.; Peng, J. B.; Cao, Y. *Chem. Eur. J.* **2007**, *13*, 7432.
13 Wang, Y. F.; Tan, H.; Liu, Y.; Jiang, C. X.; Hu, Z. Y.; Zhu, M. X.; Wang, L.; Zhu, W. G. *Tetrahedron* **2010**, *66*, 1483.
14 (a) Kawamura, Y.; Goushi, K.; Brooks, J.; Brown, J. J.; Sasabe, H.; Adachi, C. *Appl. Phys. Lett.* **2005**, *86*, 071104.
(b) Williams, E. L.; Haavisto, K.; Li, J.; Jabbour, G. E. *Adv. Mater.* **2007**, *19*, 197.
(c) Tong, B.; Mei, Q.; Wang, S.; Fang, Y.; Meng, Y.; Wang, B. *J. Mater. Chem.* **2008**, *18*, 1636.
15 Ma, B.; Djurovich, P. I.; Garon, S.; Alleyne, B.; Thompson, M. E. *Adv. Funct. Mater.* **2006**, *16*, 2438.
16 Yang, C. L.; Zhang, X. W.; You, H.; Zhu, L. Y.; Chen, L. Q.; Zhu, L. N.; Tao, Y. T.; Ma, D. G.; Shuai, Z. G.; Qin, J. G. *Adv. Funct. Mater.* **2007**, *17*, 651.
17 Sun, W. F.; Zhu, H. J.; Barron, P. M. *Chem. Mater.* **2006**, *18*, 2602.
18 Shavaleev, N. M.; Adams, H.; Best, J. *Inorg. Chem.* **2006**, *45*, 9410.
19 Kavitha, J.; Chang, S. Y.; Chi, Y. *Adv. Funct. Mater.* **2005**,

15, 223.
20 Cocchi, M.; Fattori, V.; Virgili, D. *Appl*. *Phys*. *Lett*. **2004**, *84*, 1052.
21 Yu, B. C.; Yang, X. G.; Xuan, Z. W.; Chen, X. H.; Tang, R. R. *Chin. J. Synth. Chem.* **2006**, *3*, 240 (in Chinese).
22 Liu, J.; Liu, Y.; Luo, C. P.; Liu, E. H.; Yang, Y. P.; Gan, Q.; Zhu, M. X.; Zhu, W. G.. *Chem*. *J*. *Chin. Univ.* **2006**, *27*, 1873 (in Chinese).
23 Hu, Z. Y.; Wang, Y. F.; Shi, D. Y.; Tan, H.; Li, X. S.; Wang, L.; Zhu, W. G.; Cao, Y. *Dyes Pigments* **2010**, *86*, 166.
24 Hugo, A. B.; Chris, E. F.; Kiril, R. K.; Richard, H. F.; Charlotte, K. W. *Organometallics* **2008**, *27*, 2980.

(E1012161 Zhao, X.)

